Pacific Northwest
NATIONAL LABORATORY

PNNL-34339

A Fission-like Neutron Spectrum Shaping Assembly based on D-T Generator

Development and Testing of a Low-Risk Replacement for High-Activity Neutron Sources

June 2023

Andrey V Mozhayev
Roman K Piper
Josef F Christ
Jarrod E Turner
Rodrigo Guerrero
Andrew L Maine

U.S. DEPARTMENT OF ENERGY

Prepared for the U.S. Department of Energy
under Contract DE-AC05-76RL01830

DISCLAIMER

PACIFIC NORTHWEST NATIONAL LABORATORY
operated by
BATTELLE
for the
UNITED STATES DEPARTMENT OF ENERGY
under Contract DE-AC05-76RL01830

Printed in the United States of America

Available to DOE and DOE contractors from the Office of Scientific and Technical Information,
P.O. Box 62, Oak Ridge, TN 37831-0062
www.osti.gov
ph: (865) 576-8401
fax: (865) 576-5728
email: reports@osti.gov

Available to the public from the National Technical Information Service
5301 Shawnee Rd., Alexandria, VA 22312
ph: (800) 553-NTIS (6847)
or (703) 605-6000
email: info@ntis.gov
Online ordering: http://www.ntis.gov

PNNL-34339

A Fission-like Neutron Spectrum Shaping Assembly based on D-T Generator

Development and Testing of a Low-Risk Replacement for High-Activity Neutron Sources

June 2023

Andrey V Mozhayev
Roman K Piper
Josef F Christ
Jarrod E Turner
Rodrigo Guerrero
Andrew L Maine

Prepared for
the U.S. Department of Energy
under Contract DE-AC05-76RL01830

Pacific Northwest National Laboratory
Richland, Washington 99354

Abstract

For nearly five decades, ^{252}Cf sources have been used for testing and calibration over a wide range of neutron detection devices used for nuclear safety and radiation protection. However, the vastly increased cost of ^{252}Cf sources, its short half-life, and concerns about future shortage have prompted nuclear facilities and radiological calibration laboratories that rely on high-intensity neutron sources to seek alternatives. While there appear to be no other radionuclide neutron sources that would match the ^{252}Cf performance characteristics, all of them, including ^{252}Cf, present similar concerns in terms of hazards, safety, and security. As a possible solution to this issue, the Pacific Northwest National Laboratory (PNNL) developed a low-risk, cost-efficient alternative to produce fission-like spectra based on commercially available deuterium-tritium (D-T) neutron generators. The alternative of producing a fission-like neutron spectrum without any fissionable materials or beryllium would enable the nuclear facilities across the entire complex to eliminate their reliance on high intensity ^{252}Cf sources for nuclear safety and radiation protection applications, substantially reducing risks and associated costs. This report describes efforts of designing the spectrum shaping assembly, its construction and characterization of the neutron field produced. Performance of this newly developed D-T generator based neutron field is demonstrated via calibration of a criticality detector, neutron survey instruments, and personal dosimeters verified against current standardized fields produced by ^{252}Cf spontaneous fission sources.

Acknowledgments

Funding for this effort was provided by the U.S. Department of Energy's Nuclear Safety Research and Development Program managed within the Office of Nuclear Safety (EHSS-30) within the Office of Environment, Health, Safety and Security (EHSS).

Simple Scintillator Spectrometer used for the field characterization measurements was provided by the U.S. Army Primary Standards Laboratory.

Dr. Edward Siciliano is recognized for his thorough review of this report and thoughtful feedback.

Acronyms and Abbreviations

ADE	Ambient Dose(rate) Equivalent
AmBe	Americium Beryllium
ANSI	American National Standards Institute
Bq	Becquerel
Cf	Californium
D-T	Deuterium Tritium
DOE	Department of Energy
ENDF	Evaluated Nuclear Data File
EPD	Electronic Personal Dosimeter
H*(10)	Ambient Dose Equivalent
Hp(10)	Personal Dose Equivalent
HC	Hazard Category
LSF	Low Scatter Facility
LSQ	Least Squares
MCA	Multichannel Analyzer
MCNP	Monte Carlo N-Particle
MLEM	Maximum Likelihood Estimation Maximization
NCD	Nuclear Criticality Detector
NIST	National Institute for Standards and Technology
NNS	Nested Neutron Spectrometer
NRD	Neutron REM Detector
NVLAP	National Voluntary Laboratory Accreditation Program
OSL	Optically Stimulated Luminescence
PNNL	Pacific Northwest National Laboratory
ROI	Region of Interest
ROSPEC	Rotating Neutron Spectrometer
SSA	Spectrum Shaping Assembly
SSS	Simple Scintillator Spectrometer
Sv	Sievert
TQ	Threshold Quantity

Contents

Figures

Tables

1.0 Introduction

For nearly 50 years, ^{252}Cf sources have been broadly used for testing and calibration of neutron detection devices used for nuclear safety, radiation protection, including survey instruments, criticality detectors, area monitors, and personal and area dosimeters. Reference fields produced by bare and D_2O-moderated ^{252}Cf have also been incorporated into many published American National Standards Institute (ANSI) standards, referenced in various federal regulatory codes and U.S. Department of Energy (DOE) directives. Previously, calibration of criticality detectors and high-range instruments (e.g., 20 mSv h^{-1} and above) relied on high-activity ^{252}Cf sources available for relatively low cost through the ^{252}Cf Loan/Lease Program at Oak Ridge National Laboratory. In 2009, funding for the DOE production of ^{252}Cf was discontinued, which resulted in the Loan/Lease Program closure in 2012. In response to the continued demand for ^{252}Cf, several private sealed source manufacturers formed a consortium to continue funding U.S. production and purification of ^{252}Cf, thus preserving the availability of this important isotope. However, as a result, the cost of procurement for an encapsulated high-intensity ^{252}Cf source drastically increased. By 2016, the cost was nearly 15 times more than in 2002. The relative increase was even larger compared to the cost of obtaining encapsulated sources through the former ^{252}Cf Loan/Lease Program. For nuclear facilities and radiological calibration laboratories that depend on high-intensity sources (e.g., neutron emission rate above 10^9 s^{-1}), the marked increase in cost is prohibitive[1], prompting the need for an alternative.

Americium-Beryllium (AmBe) compound is another type of radioisotope source that has been widely used by both various industries and research organizations. With the half-life of 432 years, no frequent source replacements due to decay are envisioned, however, the maximum intensity of a 40GBq commercially available encapsulated AmBe source is $5 \cdot 10^7$ s^{-1}. Thus, achieving a neutron emission rate of 10^9 s^{-1} would require bundling twenty of these sources containing approximately 120g of ^{241}Am in total and a fivefold amount of beryllium. Disregarding the cost[2] comparable to ^{252}Cf of similar intensity such a quantity could not physically be considered and used as a single “point” source.

While there are no other radionuclide neutron sources that would potentially match the ^{252}Cf performance characteristics, all of them, including ^{252}Cf, present similar concerns in terms of hazards, safety, and security.

On the other hand, the development of compact electronic neutron generators has matured to a level where neutron yields rival those of ^{252}Cf sources. Various commercially available generators may present viable options in terms of reduced cost[3] and risks and be considered potential alternatives for the facilities. Substantial cost savings come with the price of a new neutron generator being a mere fraction of that for a ^{252}Cf source of same intensity and a typical

[1] The cost of an encapsulated ^{252}Cf source with neutron emission rate of $6 \cdot 10^9$ s^{-1} approaches $3 million. With a half-life of 2.646 years, such ^{252}Cf sources need to be replaced every 8-15 years, depending on application.

[2] The cost of a single 590GBq AmBe source exceeds one hundred thousand dollars, whereas the price of a maximum 740GBq AmBe source would exceed one hundred fifty thousand dollars.

[3] The cost of a new neutron generator ranges from $100K up to $400K, depending on the output (10^8 – 10^{10} n/s) and the system complexity. The consequent replacements of the neutron tubes require approximately 25% of the corresponding cost for the new system.

working life of a neutron tube is about 1000 hours or longer, which may be interpreted to approximately 3 years of active use.

Although a D-T generator will not be excluded from a facility's radioactive material inventory, unlike radionuclide sources in special form encapsulation, the amount of tritium contained in most neutron generator tubes is less than a per mille of the threshold quantity (TQ) for Hazard Category 3 (HC3) (Table 1-1 in DOE-STD-1027-2018). Whereas source manufacturers typically establish the working life of radionuclide sources not to exceed 15 years, in the case of AmBe and ^{252}Cf sources, potential internal pressure buildup due to alpha decay may require periodic evaluation of the source integrity and mitigation of associated hazards. If not excluded, a single AmBe source of relatively low yield ($6 \cdot 10^6$ n/s) will still exceed the ^{241}Am HC3 TQ. (Table 1-1 in DOE-STD-1027-2018). Even at such low intensities, both AmBe and ^{252}Cf neutron sources contain accountable quantities of nuclear materials and are subject to corresponding Safeguards requirements (DOE O 474.2, Nuclear Material Control and Accountability), whereas D-T neutron generators contain less tritium than a typical Exit sign (Chichester and Simpson 2003) (below a per mille of the reportable quantity).

While neutron generator systems have many advantages, there are also challenges. One of them is associated with the difference between narrow mono-energetic neutrons produced by generators and broad energy neutron fields produced by radionuclide sources and especially those found in the nuclear workplace. However, the energy profile of neutrons from deuterium-tritium (D-T) reactions may be "shaped" by complementing the generators with specifically designed convertors. Various designs of shaping assemblies have been explored and even built, however, some of installations use depleted uranium as a primary convertor taking advantage of fission induced (Chartier, Posny and Buxerolle 1992), (Nunes, Cross and Waker 1997), (Koltick, McConchie and Sword 2008). However, such configurations, in opposite, elevate risk and safety concerns.

The investigation of possible concepts for creating broad energy spectra using neutron generators to replace the bare and D_2O-moderated ^{252}Cf standards without using depleted uranium, beryllium and heavy water was supported under the PNNL Laboratory Directed Research and Development Program (A. V. Mozhayev, R. K. Piper, et al. 2016). Two-year-long simulations-based studies resulted in several spectrum shaping assembly (SSA) design concepts aiming to replicate different target spectra (A. V. Mozhayev, R. K. Piper, et al. 2017), (Piper, et al. 2017). One of the developed concepts comprised of a series of concentric bismuth cones surrounding the generator head, completed with a tungsten-tipped core plug made of lead was intended to create a surrogate fission-like spectrum with no fissionable materials. This report describes the concept design adaptation, its construction and testing for applications of instrument and dosimetry calibrations.

2.0 Designing Spectrum Shaping Assembly (SSA): From Concept to Lab-Scale Prototype

The originally conceived configuration for shaping a monoenergetic 14 MeV neutrons into a fission-like spectrum is shown in Figure 1. To accomplish such a SSA configuration in real life required making several changes dictated by the established project schedule, available resources, and capabilities. The effects of these changes made to the original design concept were evaluated via multiple simulations using the following metrics: total fluence preservation [$\Phi_{total}/\Phi_{bareDT}$], average energy of the shaped spectrum below 12 MeV [$E_{av<12}$] and remaining fraction of 14 MeV neutrons [Φ_{14}/Φ_{total}].

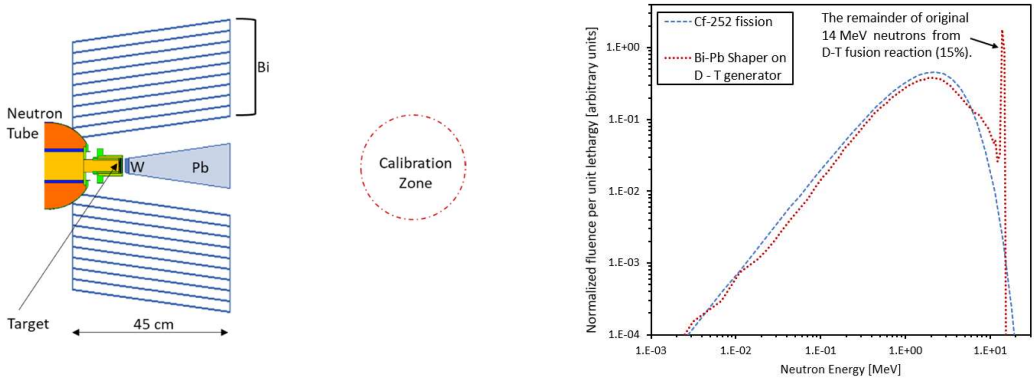

Figure 1. The original SSA concept to convert D-T generated neutrons into a fission-like spectrum (Left). Simulated spectrum utilizing this concept compared to ^{252}Cf (Right).

2.1 Materials

The original conceptual SSA design consisted of ten coaxial truncated cones of 3mm thick bismuth. However, pure bismuth metal was found too brittle to serve as the structural material. Using it in the form of encased powder was considered but discarded as unfeasible for two reasons: the possibility of breaching encasement during installation and additional safety measures that would be required for manufacturing and further use related to the flammability of bismuth powder. Comparison of the original design using cones made of bismuth, lead, and lead-bismuth eutectic (LBE) alloy showed that lead provided higher fluence preservation and the lesser fraction of un-scattered 14 MeV neutrons. However, its spectrum of scattered neutrons was softer than bismuth, whose spectral shape was the closest to the targeted ^{252}Cf fission energy distribution. The resulting spectra are compared in Figure 2. As expected LBE spectral fluence characteristics fall between those of lead and bismuth. Also, LBE alloy has significantly lower melting temperature[1] comparing to its pure constituents, suggesting a simpler casting process. Thus, LBE was considered as an optimum material to proceed. From the standpoint of practicality, the thickness of cones was doubled and hence their number was reduced from ten to five.

[1] Melting temperature of lead bismuth eutectic is 124°C, whereas lead melts at 328°C, and bismuth melts at 271°C.

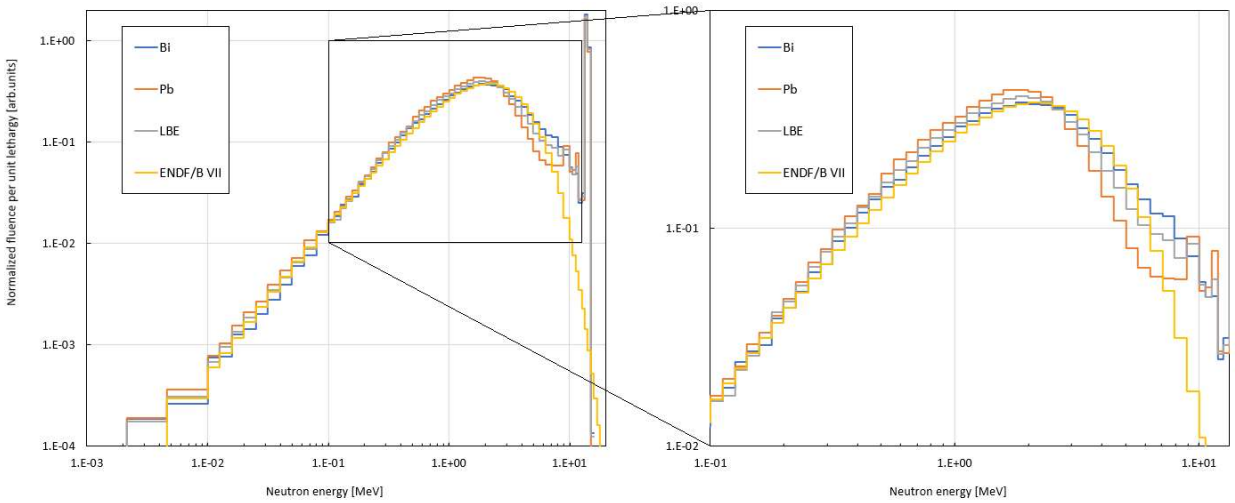

Figure 2. Comparison of spectra generated by the ten-cone shaper made of Pb, Bi and LBE

2.2 Practicable Geometries

The truncated cones were effective as a concept, but considering their size and weight, could be challenging to fabricate and easily damaged or deformed during handling or installation. Therefore, to simplify fabrication and further handling the nested cones were replaced with flat panels. Extensive modeling iterations resulted in two favorite designs for the spectrum shaper panels: nested pyramidal shells or the turbine-like fins as shown in Figure 3. The efficacy of the designs was evaluated via Monte Carlo simulations using the code MCNP6 Version 1.0 with ENDF/B-VII.1 cross-section libraries (Goorley, et al. 2012). Key parameters are compared in Table 1.

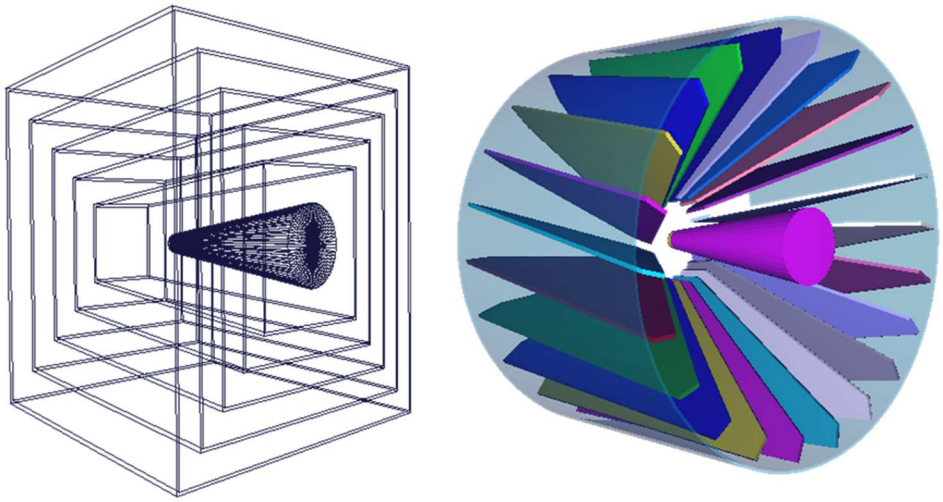

Figure 3. SSA flat panel designs: pyramidal shells (left) and turbine-like fins (right).

Table 1. Comparison of conic to flat panel spectrum shaper designs

Parameter	Original Cone Design	Nested Pyramid Panels	Turbine-Fin Panels
Fluence preservation, [$\Phi_{total}/\Phi_{bareDT}$]	42%	48%	35%
Average energy <12MeV [$E_{av<12}$], MeV	2.34	2.21	2.24
Remaining 14MeV fraction [Φ_{14}/Φ_{total}]	14.4%	14.7%	13.1%

While all fins in the turbine-like design were the same shape and size making their fabrication simpler, the nested pyramidal shells provided better performance. In the next step, various shapes of pyramid bases were considered: square, hexagon and octagon. To allow for assembly and installation of the SSA without using a hoist, the weight of individual components was limited to be manageable by a single person. That limitation led towards increasing the number of facets (pyramid sides), but on the other hand, a larger quantity of individual components would necessitate a more complicated frame that kept them in place. As a result, the hexagonal shape was selected to provide an optimum between the weight limitation and the frame complexity. The heaviest LBE panel was to weigh about 12 kg. The frame was to be made of aluminum to reduce unwanted scatter and minimize potential activation issues. The inscribed diameter of the SSA was increased to accommodate for the wide head (tube) of the Thermo D711 neutron generator. The design rendering with estimated key parameters is shown in Figure 4 and the resulting spectrum is compared to the concept and ^{252}Cf fission in Figure 5.

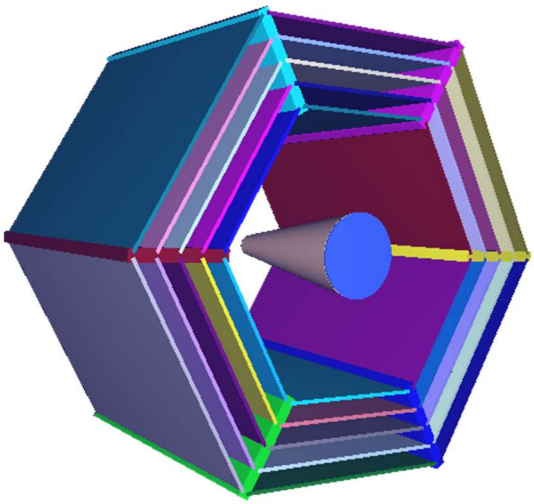

Hexagonal Assembly

[$\Phi_{total}/\Phi_{bareDT}$] 46%

[$E_{av<12}$], MeV 2.2

[Φ_{14}/Φ_{total}] 10.8%

Figure 4. Hexagonal assembly design

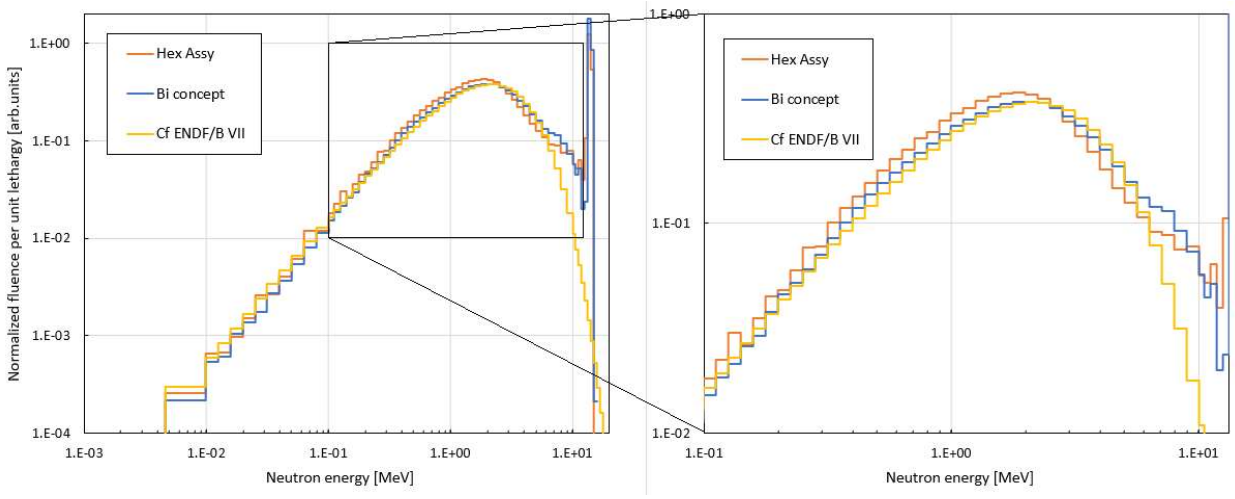

Figure 5. Comparison of spectra generated by the hexagonal assembly, the concept and ^{252}Cf.

2.3 Framing and Supporting Structure

The conceptual SSA was modeled as a stand-alone object in a air-filled space, whereas a realistic prototype needs to be securely connected and situated in the room near the head of the existing generator. For the realistic system, the aluminum exoskeleton was designed to form the assembly complete with the hexagonal scattering plates and the conical plug. Six panels, slotted for holding scattering plates, were bolted between front and rear hexagonal plates forming a rigid structure of the main assembly. The plug holder consisted of three beams welded to the center-aligning ring on the inside (i.e. near the generator target) and with the opposite ends bolted to the front hexagonal plate. The solid lead plug was to be compounded of three truncated conical pieces. A tungsten tip, planned nearest the generator target to provide effective degradation of the 14 MeV fluence, was transformed to become a cover plate fastened to the front hexagonal panel to essentially keep the conical lead plug in its holder. The horizontal slotted panels had extended coupling surfaces to be mounted onto the supporting structure.

The assembly supporting structure was to comprise two masts erected on a base frame – all built with T-slotted aluminum profile. It was envisioned that the scatterer will be oriented vertically for loading LBE plates and then the complete assembly rotated and carefully moved over the generator tube. To accommodate that transition, the entire supporting structure is to be sliding on rails. Later an additional bracket that would vertically slide on the masts was introduced into the design to ease loading the SSA with LBE plates. It would be loaded at its lower position – approximately at 1 meter from the ground and then rotated and elevated with a car jack by approximately 50 cm to align with the generator head height. The growing mass and complexity of the entire structure required increasing the rigidity of the base and accounting for proper weight distribution between load bearing beams of the irradiation facility mezzanine. The evolution of the supporting structure designs is illustrated in Figure 6.

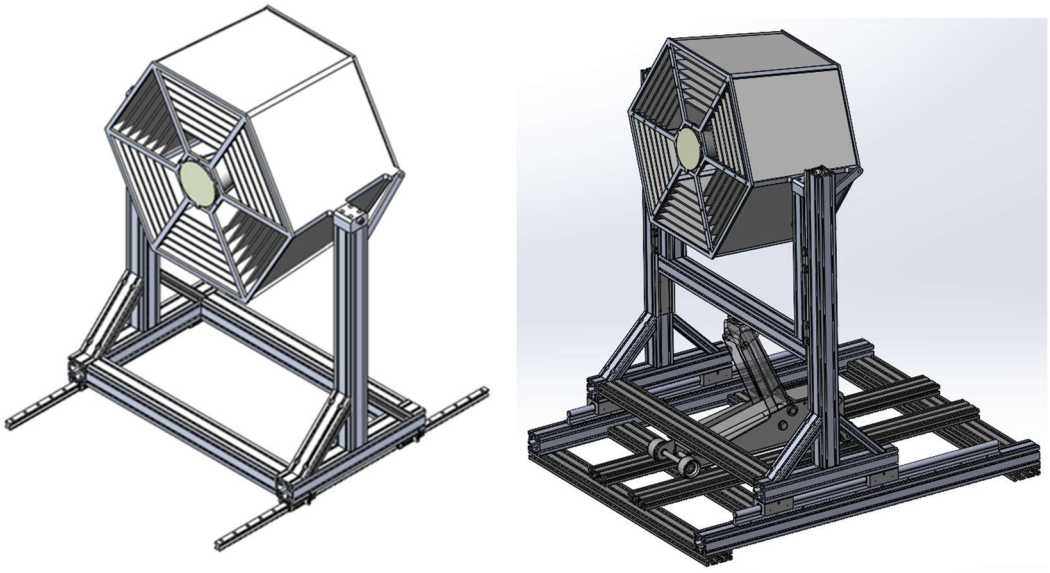

Figure 6. Evolution of the supporting structure.

2.4 Final Design

Two shorter inner layers of scattering plates were added in order to compensate for the decreased efficacy of the shaping assembly caused by the enlarged diameter accommodating dimensions of the neutron generator head. Thus, the final SSA ended up having 42 plates distributed in seven coaxial layers.

Browsing in the smelters market and contacting different manufacturers revealed a sad reality - the actual cost of fabricating LBE components could be higher than the total budget of the project. Apparently, processing LBE alloy would contaminate production lines of pure lead with unwanted bismuth, or vice versa, and hence would require afterwards the extensive cleaning of fabrication equipment at a disproportionally high cost comparing to such a small batch of material needed for the project. As a result, the project elected to proceed with essentially the only affordable and previously evaluated option – using lead as a material for the scatterer plates with their thickness reduced 6 mm to 5 mm.

The need for another design revision became obvious while situating the entire structure at the mezzanine in the low scatter facility (LSF). For proper positioning and alignment with the DT generator, the distance between the rails and hence the masts had to be reduced. This led to a complete redesign of the structure with the assembly support bracket sliding in between split masts. The final design of the assembly and support structure shown in Figure 7 with the total mass approaching 635 kg underwent thorough engineering evaluations for seismic and structural integrity prior to being approved for installation at the mezzanine.

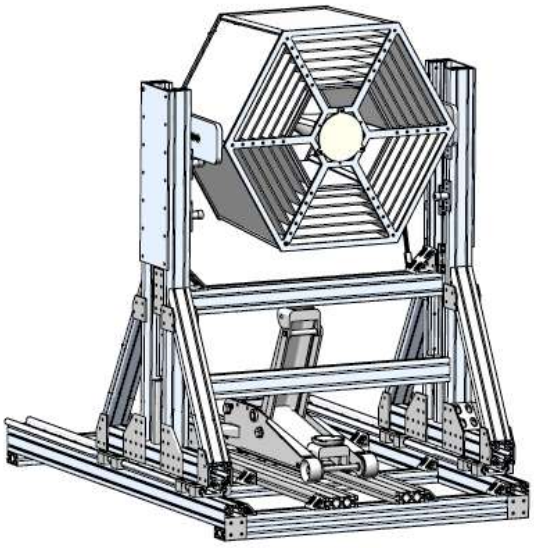

Figure 7. The final design of the SSA assembly and support structure.

2.5 Fabrication and Installation

Both lead plug and plates were fabricated per design specifications by a commercial manufacturer selected through competitive bidding process. To prevent oxidation all lead pieces were supplied already painted. The PNNL shop fabricated the tungsten cover plate, aluminum slotted panels, the plug holder as well as hexagonal front and rear plates from acquired stock materials. All T-slotted aluminum profile parts for the support structure were purchased precut per drawings.

The entire assembly and support structure were first constructed on the floor in a spacious room to test fit different parts and make necessary adjustments. Slight variations from the initial drawings were realized. Flat lead plates had to be curved out to fit into corresponding spacing between holder panels. The convex form of the originally flat plates transformed the appearance of the scatterer to resemble the circular layers (truncated cones) of the original concept. A minor difference in the solid angles of the fabricated conical lead plug and its holder was compensated by filling a 6 mm gap with a corresponding lead disk on the tip of the plug (i.e. near the generator target and similar size spacers to the base of the holder. After the adjustments were made and all sliding, elevational and rotational movements were tested, the erected assembly was dismantled into manageable pieces and transported to the LSF for installation.

The LSF is a large irradiation room with relatively low and easily quantified albedo for the neutron calibrations. The room has over one-meter-thick concrete walls and measures approximately 15 x 10 x 9 meters. Both the D-T generator and one of the ^{252}Cf source irradiation stations are mounted on a raised aluminum platform, the mezzanine, located approximately at the geometrical center of the room. A pneumatically driven “rabbit” system is used to move sources from their storage locations to any of the irradiation stations. The location for placement of the spectrum shaping assembly (SSA) prototype in the LSF is shown in Figure 8.

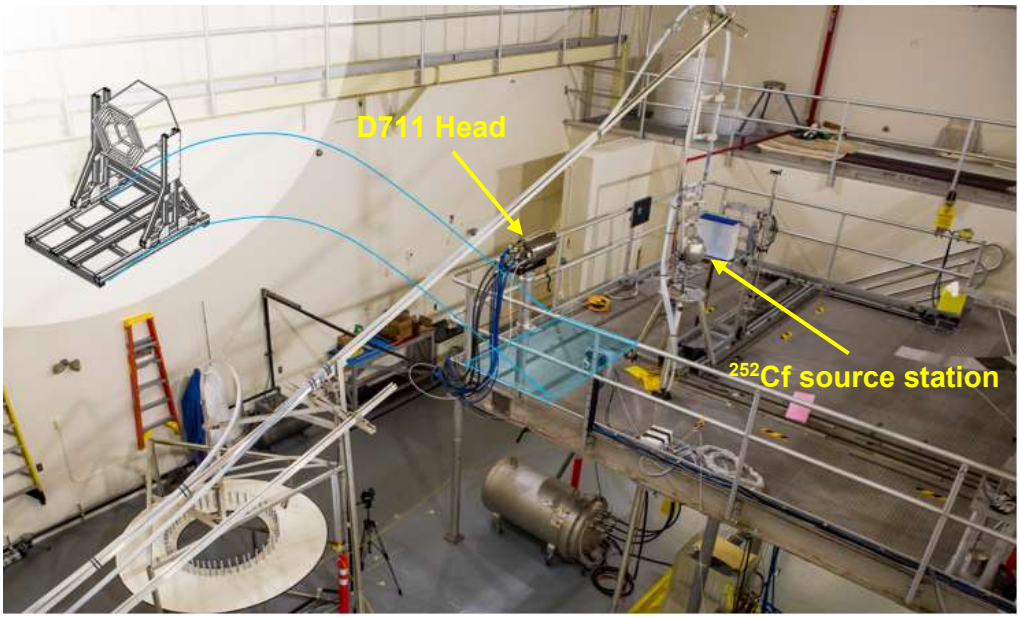

Figure 8. Location of the SSA prototype on the mezzanine in the LSF.

Figure 9 shows the SSA prototype as installed over the neutron generator head on the mezzanine. The installation of the entire structure was performed essentially by a single person in less than four hours and its dismantling, after a month of testing, required only half of that time.

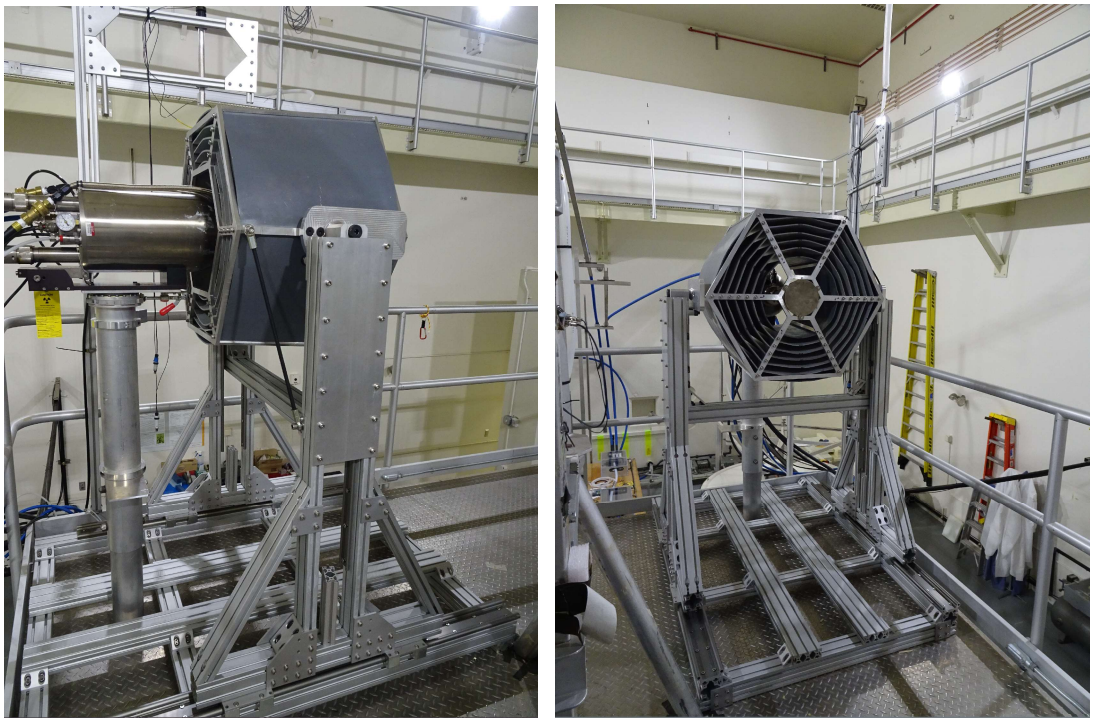

Figure 9. SSA prototype installed over the neutron generator head on the mezzanine in the LSF

3.0 Field Characterization

The ^{252}Cf reference field in the LSF is a well-established calibration capability that is provided within the PNNL scope of NVLAP accreditation (Laboratory Scope 105020-0). Traceability is established via calibration of the isotopic source total emission rate as defined by the NIST Manganous Sulfate bath method, where the source is placed within its almost total encapsulation employed under normal use. The emission rate from the source typically is used to define the dose equivalent at a reference calibration point as in a vacuum (i.e., free field). However, during such use, the source is pneumatically located at an irradiation station comprised of a double walled aluminum tube near the center of the facility. In addition to the neutrons directly emitted from the source, instruments and dosimeters tested in the facility are also exposed to neutrons scattered from the surrounding aluminum tube, ambient air and the facility structures (walls, ceiling, floor, etc.). The additional estimated influence of these indirect neutrons reaching the instrument or dosimeter generally rely on calculations via Monte Carlo simulations. The dose value from these indirect neutrons is appended to the dose value from the direct neutrons to arrive at a total neutron dose. Therefore, calibration measurements or reference irradiations are typically conducted at distances between 50 cm and 100 cm as an optimum to minimize the indirectly scattered contribution and the angular variability of neutron emission at proximity to the source. Similarly, the surrogate field established in this project will reflect full scattering conditions and angular distributions at the reference point established at 100 cm from the generator target.

3.1 Simulation model

Initially, in the process of a designing prototype all simulation models of the SSA were placed in a simple, air-filled space without accounting for the indirect neutron scattering from the actual experimental environment. To simulate a realistic spectrum at the reference dose point a detailed model of the as- built prototype shown in Figure 10 was coupled with the previously developed model of the D711 generator head and the source term (A. V. Mozhayev, R. K. Piper, et al. 2017) and situated in a realistic model of the LSF environment, which included various pedestals and supporting structures, the mezzanine platform and concrete walls, ceiling, and floor. In this model of the LSF, the designated reference dose point was represented as 1 cm-thick disk of 20 cm in diameter with its axis aligned with the axis of the generator head. The volume was then subdivided into the central cylinder of 10 cm in diameter and surrounding ring 5 cm thick. The cylindrical core was intended to estimate neutron fluence representative to probes of survey instruments, whereas the entire disk would correspond to dosimeter placement zone. Neutron fluence [cm^2 per source neutron] was tallied as the sum of track lengths in the corresponding volume (MCNP tally type F4). Simulations were run for 10^9 histories resulting in relative statistical errors of approximately 0.1% for total neutron fluence. The resulting spectrum is plotted in Figure 11 against the simulated fluence energy distribution at 100 cm from a ^{252}Cf source in the room and the original ^{252}Cf fission spectrum. The preservation of the total fluence comparing to the bare DT generator is 54.7% (with the room scatter included in both cases). The fraction of un-scattered 14 MeV neutrons appears to be twice less than predicted in the concept, however, thermal and intermediate components of the neutron spectrum generated by the SSA prototype appear to be relatively higher comparing to the produced by ^{252}Cf source. The average energies of the primary broad peak [from 0.01 to 12.6 MeV] are 1.89 and 1.87 MeV for the SSA prototype and bare ^{252}Cf, respectively. The anticipated shift of the peak towards lower energy due to replacement of bismuth with lead seems to be compensated by a continuum of scattered neutrons between 8 and 12 MeV.

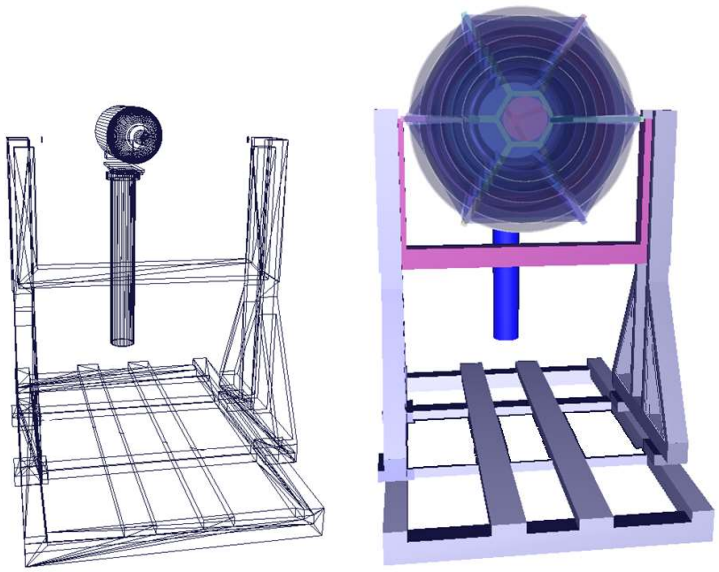

Figure 10. 3D rendering of the generator head and the spectrum shaping assembly

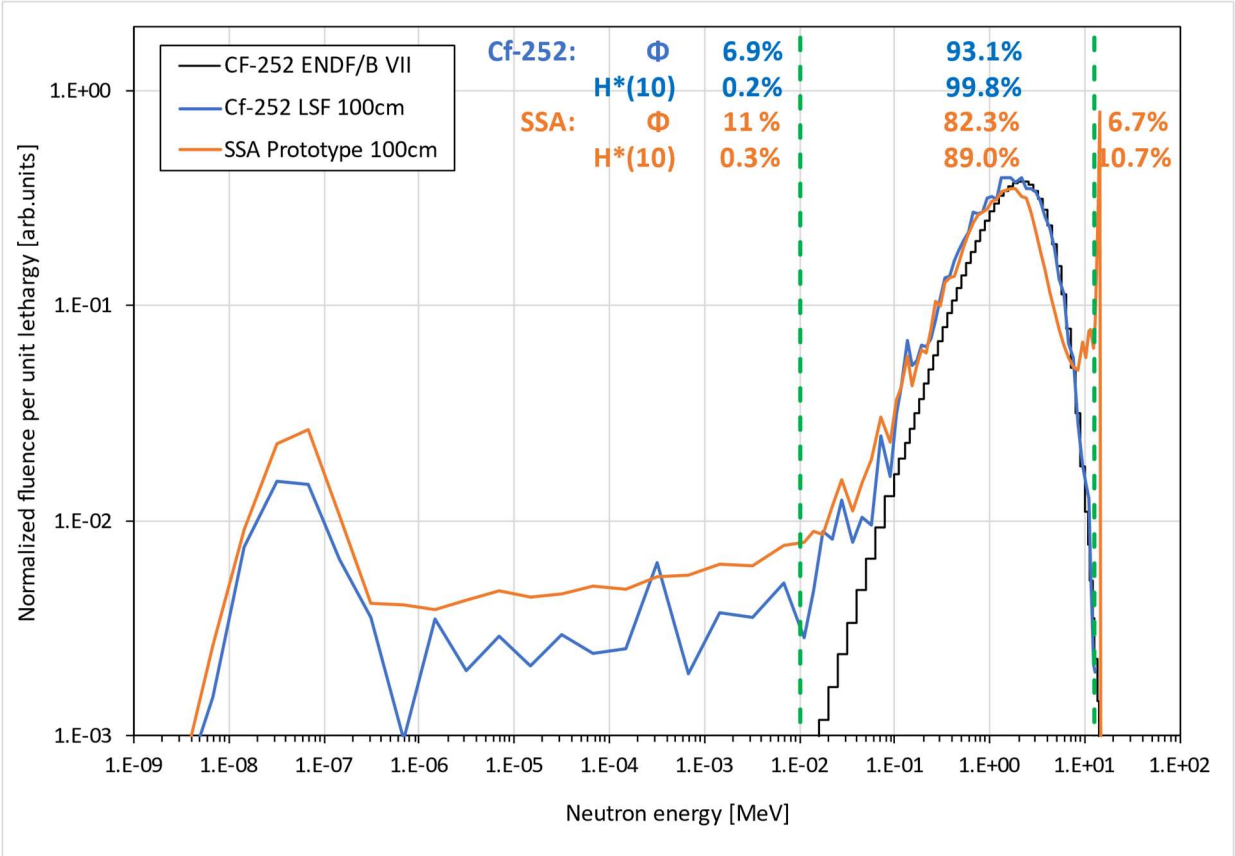

Figure 11. Normalized spectra produced by ^{252}Cf and SSA Prototype at 100cm in the LSF.

Fluence-to-dose-equivalent conversation coefficients calculated for reference dose point of the field produced by bare ^{252}Cf source, bare DT generator and SSA prototype are presented in Table 2.

Table 2. Calculated fluence-to-dose-equivalent conversion coefficient for the reference point.

	Bare ^{252}Cf	Bare DT generator	SSA prototype
Ambient dose equivalent, H*(10) [pSv.cm^2]	347	472	333
Personal dose equivalent, Hp(10) [pSv.cm^2]	360	496	347

3.2 Field Calibration Measurements

Unlike radionuclide sources, which emission rate can be accurately determined at any time (after applying a proper decay correction), the neutron output of electronic generators could fluctuate even at steady current and accelerating voltage. Therefore, the actual neutron production needs to be monitored. A custom-composed detector consisting of a Reuter Stokes ^{235}U fission chamber (Model RS-P6-0805-134) inside a cylindrical polyethylene moderator (9 inch in diameter and 10 inch long) was used to continuously record counts every ten seconds during the DT generator operation. The stability of the monitor performance was checked by periodic measurements of a ^{252}Cf source. Repeatability of source check measurements conducted from December through February was 0.7% (one standard deviation). The intensity of the neutron field produced by the generator at the time of testing survey instrument or dosimeter irradiations could be estimated by normalizing the monitor response to the time of field calibration measurements. The neutron fields produced by the bare generator and equipped with the SSA prototype were measured using a multi-moderated (nested neutron) spectrometer, a rotating (proton-recoil) spectrometer, and a tissue equivalent proportional counter.

3.2.1 Nested Neutron Spectrometer

The nested neutron spectrometer (NNS) (Dubeau, et al. 2012) represents a reincarnation of Bonner-sphere spectrometers (Bramblett, Ewing and Bonner 1960). It uses a 2 atm ^{3}He detector and different size polyethylene moderators in the form of cylindrical shells placed inside one another like Matryoshka dolls. Depending on the field intensity the NNS can operate in either pulse or current mode enabling to perform measurements in fields of various intensity. The application software allows either to generate a guess spectrum or to load one defined by the user. The spectrum deconvolution can be performed by two methods – Least Squares (LSQ) and Maximum Likelihood Estimation Maximization (MLEM). Prior to characterization of the generator-produced fields the spectrometer was calibrated by measurements of a reference field at 50 cm from ^{252}Cf. The energy distribution simulated for that measurement geometry was used as a guess spectrum for unfolding acquired data. Results obtained using both LSQ and MLEM methods after adjustment of the detection sensitivity coefficient are presented in Table 3. NNS spectrum measurements of the both generator-produced fields were performed at 100 cm from the edge of target cap (approximately 65.5 cm from the front of the SSA prototype). Figure 12 illustrates NNS measurements of the neutron field produced by the bare D-T generator with the detector placed in the largest moderating cylinder on the left and on the right the SSA prototype using the bare detector. The measured data were unfolded using both LSQ and MLEM methods based on simulated guess spectra. Measured spectra and results of the bare

D-T generator field are shown in Figure 13. Measured spectra and results of the SSA prototype field are presented in Figure 14.

Table 3. NNS Performance

Parameter	Accepted Knowledge	LSQ	MLEM
Total fluence rate [$s^{-1}.cm^{-2}$]	$1.52 \cdot 10^4$	$1.49 \cdot 10^4$	$1.51 \cdot 10^4$
Ambient dose rate equivalent, [uSv/h]	$2.01 \cdot 10^4$	$2.02 \cdot 10^4$	$2.03 \cdot 10^4$
Fluence-to-ADE conversion coefficient [$pSv.cm^2$]	368	376	372

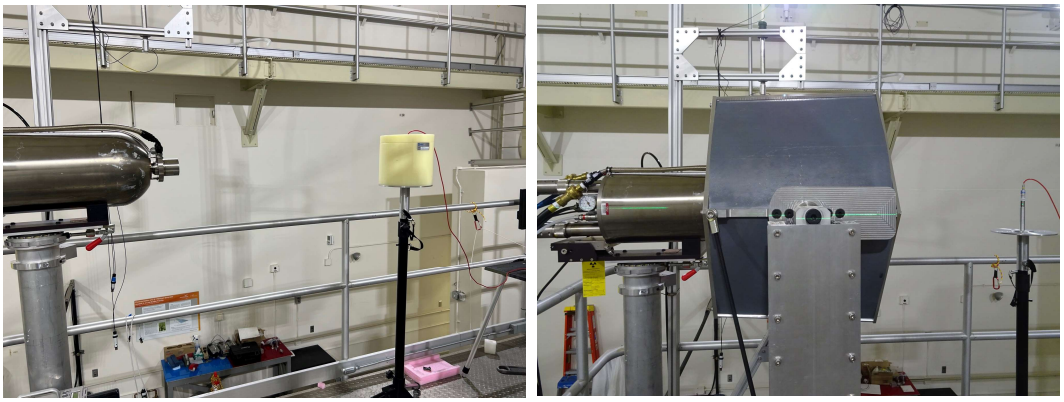

Figure 12. NNS measurements of generator produced fields: bare (left) and SSA (right).

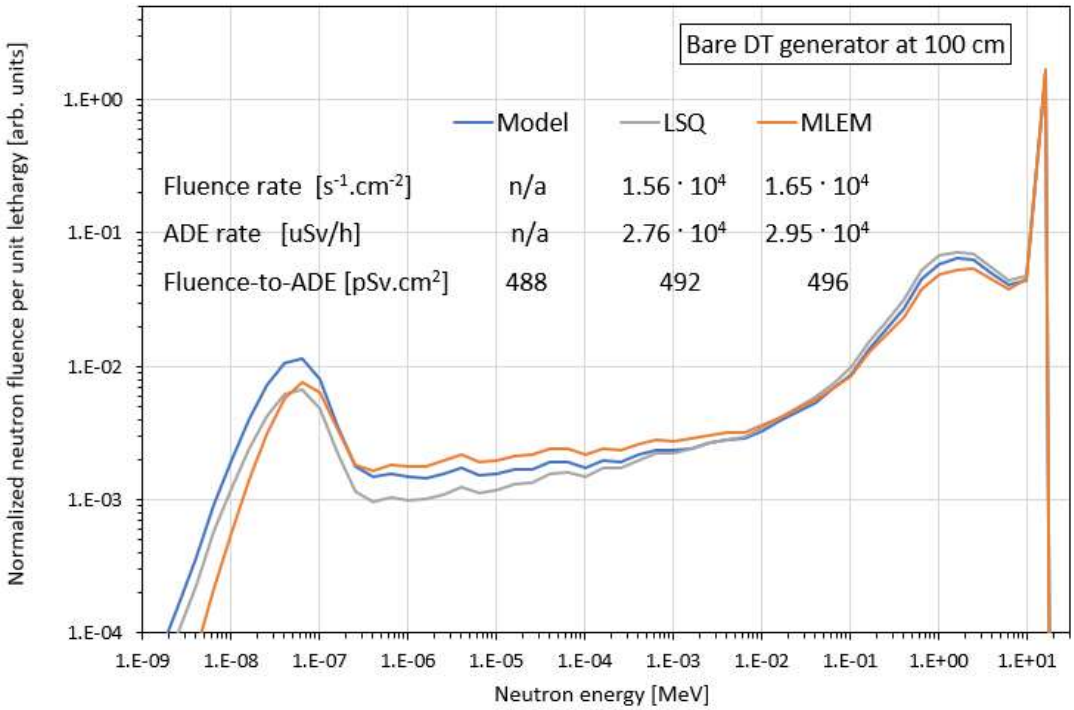

Figure 13. NNS measurement results for the bare D-T generator.

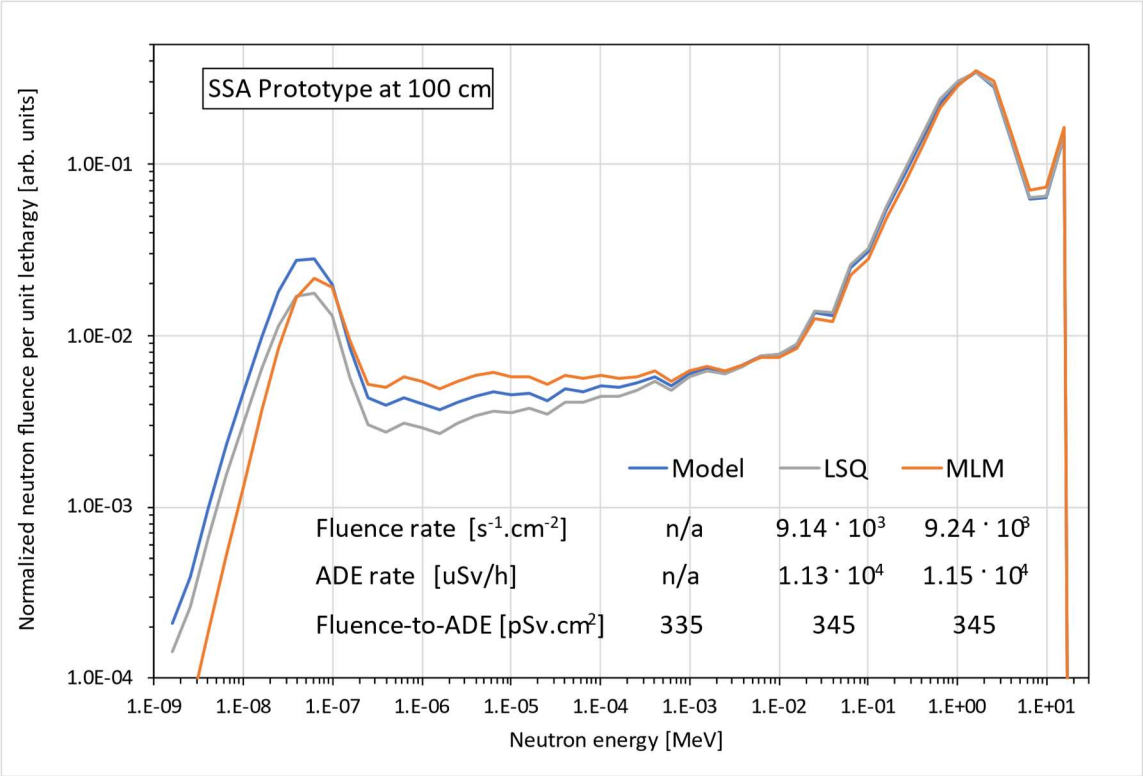

Figure 14. NNS measurement results for the SSA prototype.

3.2.2 Rotating Neutron Spectrometer

The rotating neutron spectrometer, ROSPEC, consists of six spherical gas-filled proportional detectors that rotate around a common axis. A base ROSPEC neutron spectrometer (Ing, Clifford, et al. 1997) uses 4 proton-recoil proportional counters of various diameters filled with hydrogenous gas at different pressures that are optimized to detect neutrons with energies ranging from 50 keV to 4.5 MeV. The spectrometry system used in this work is additionally supplemented by a pair of bare and boron-covered ^{3}He detectors, which extend the lower detection energy range to thermal neutrons as well as the simple scintillation spectrometer (SSS) expanding the measured energy range of ROSPEC up to 17 MeV (Ing, Djeffal, et al. 2007). The measured pulse-height distributions collected with proton-recoil detectors are analyzed by the built-in unfolding software based on Spec4 code (Benjamin, et al., 1968), (Kemshall, 1973). Spectrum unfolding starts with the highest energy region and proceeds to the next below accounting for corresponding influence (down scatter) of already analyzed higher energy neutrons.

The performance of the ROSPEC/SSS system was verified by measurement of the neutron field produced at 100 cm from a NIST-calibrated ^{252}Cf source. The measured spectrum was unfolded, and then compared to a simulated spectrum. Measured fluence rate and ambient dose rate equivalent agreed with the accepted values within 1% demonstrating good performance of the ROSPEC/SSS system. Spectra and the neutron field paraments are compared in Figure 15.

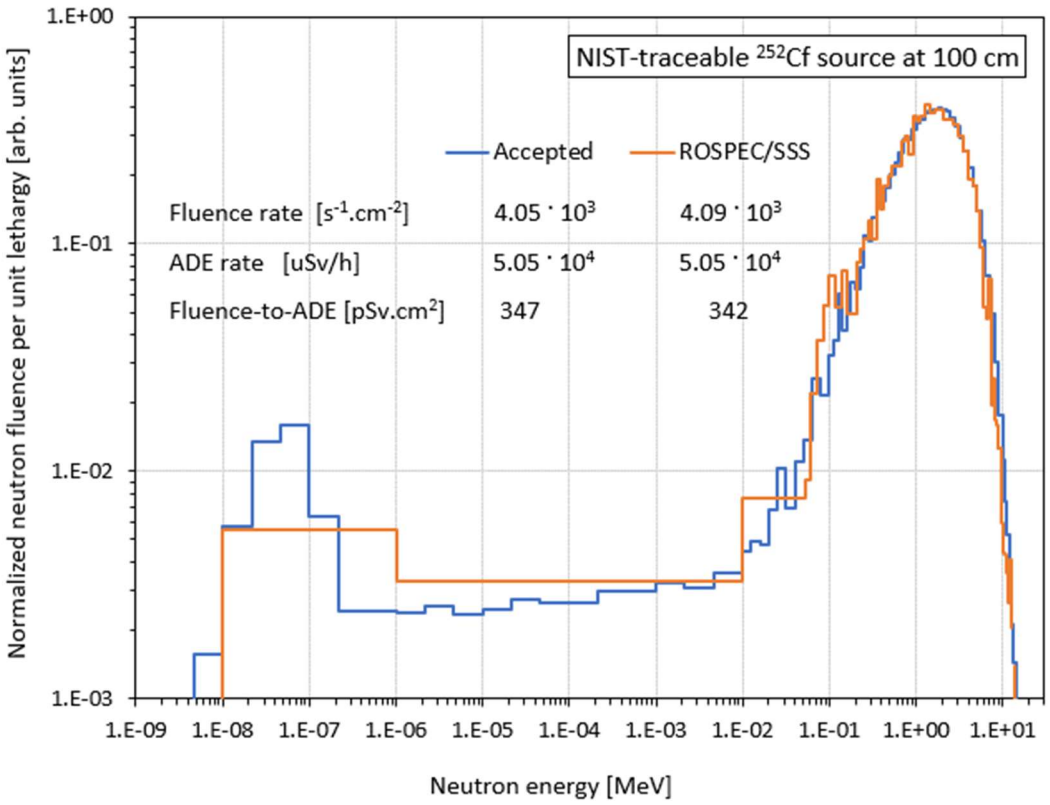

Figure 15. ROSPEC/SSS measurement of NIST-traceable ^{252}Cf source.

The ROSPEC/SSS system has been considered the state-of-the-art high resolution neutron spectrometer intended for radiation protection applications. However, the ROSPEC transmission buffer has the rate threshold of 1600 data pairs per second, that in turn defines the maximum intensity of the field that can be reliably measured. Unfortunately, the intensity of the both generator-produced fields at 100 cm from the target cap, was high enough resulting in count rates exceeding the ROSPEC data transmission capacity. Thus, obtained measurement data had to be treated with caution. Figure 16 illustrates measurements of the neutron field produced by the SSA prototype with the ROSPEC and SSS probe. In addition, the ion source of the D-T generator produces intensive X-ray radiation, which provides significant signal interference for the low-pressure hydrogen filled proportional counter. As a result, the analysis of data acquired in the bare generator field failed to produce combined ROSPEC/SSS results, and hence only SSS measurements were used for quantification of the field. Luckily, the fraction of neutrons with energies below 4MeV was expected to be insignificant. The measurement results for the bare D-T generator field obtained with SSS are presented in Figure 17. Absolute values of fluence rate and ambient dose equivalent derived from ROSPEC/SSS measurements of the SSA prototype field were obviously lower than those obtained earlier with NNS. The observed difference was attributed to data losses due to the rate threshold of the ROSPEC transmission buffer. However, the normalized spectrum appeared to agree with the simulated and the fluence-to-dose equivalent conversion coefficient calculated from measured values matched the one obtained from simulations. The ROSPEC/SSS measured spectrum and data for the SSA prototype field are shown in Figure 18.

Figure 16. The SSA prototype field measured with ROSPEC (left) and SSS probe (right).

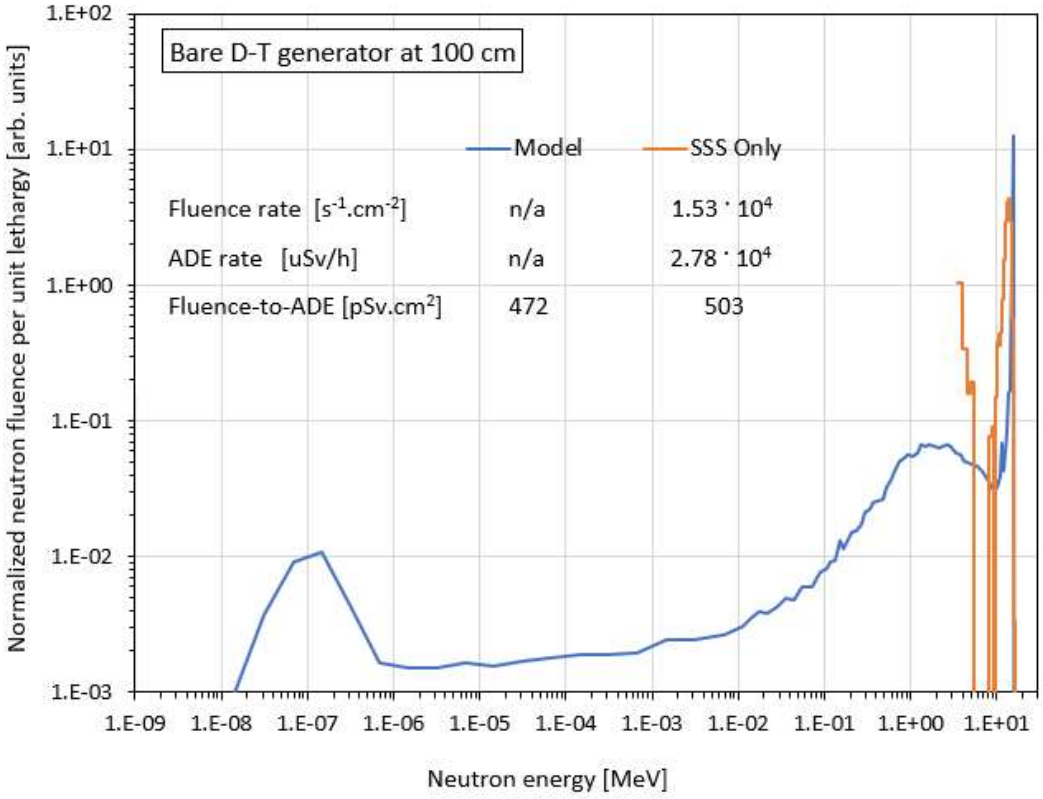

Figure 17. Bare D-T generator field at 100 cm measured by SSS Only.

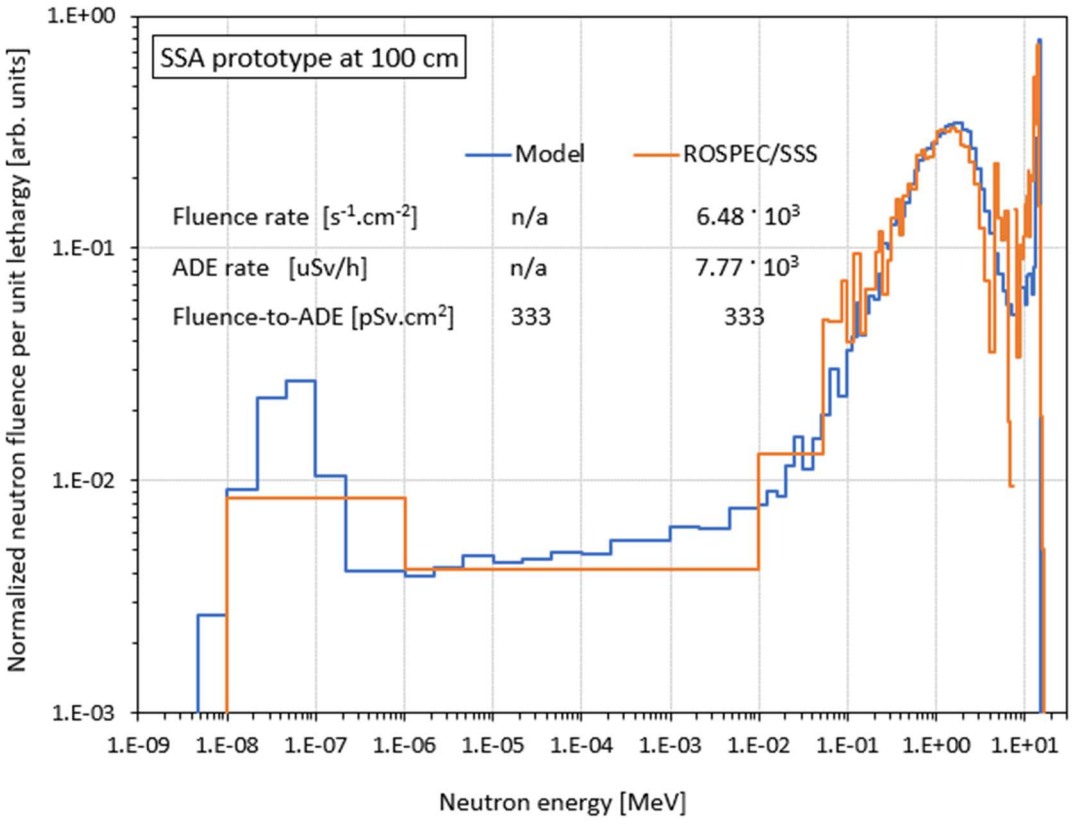

Figure 18. ROSPEC/SSS measured SSA prototype field at 100 cm from the target cap.

Additional ROSPEC/SSS measurements at larger distances from the generator target were performed in order to determine the fraction of the countrate lost due to the data transmission threshold. Normalized results of the measurements are compared in Figure 19Figure 19 to corresponding normalized values predicted by simulations. The difference observed between data points at 100 cm provides an estimate for correction of the measurement results.

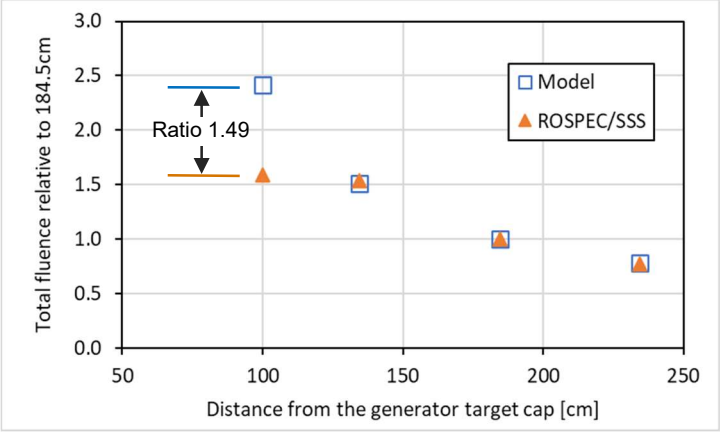

Figure 19. Relative total fluence of the SSA prototype field.

3.2.3 Tissue Equivalent Proportional Counter

REM-500 survey meter is based on a Rossi-type spherical proportional counter, with a 60mm in diameter with an A150 wall thickness of 1.2mm (Health Physics Instruments 1998). The detector volume is filled with propane to a nominal pressure of 13.3 mmHg, representing 2 µm of tissue. The detector employs a built-in 256 channel analyzer to resolve lineal energy distribution. Response in each channel is corrected by an energy-specific ambient dose-equivalent correction coefficient. The manufacturer's stated neutron energy sensitivity ranges from 70 keV to 20 MeV. Verification measurements of the dose rate produced at 100 cm from a NIST-calibrated ^{252}Cf source showed a negative bias of 6% and hence the corresponding correction was applied to following results of REM-500 field characterization. Measurements of generator produced fields and average sensitivity corrected results are shown in Figure 20.

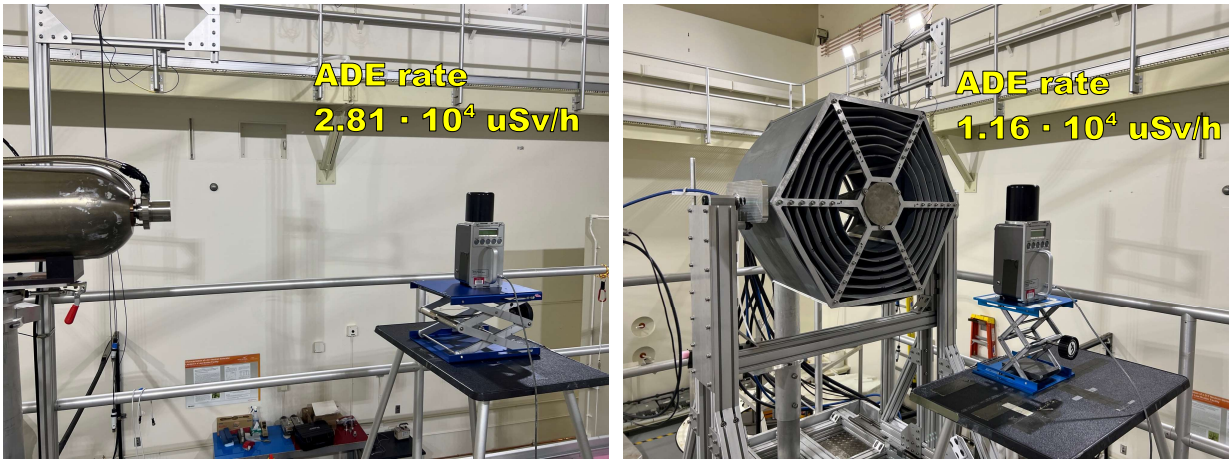

Figure 20. REM-500 measurements of generator-produced fields: bare DT (left) and SSA (right).

3.2.4 Accepted Fluence and Dose rate Values

Three instruments used for the field characterization are based on different measurement principles and hence provide robust estimates of the only common reported parameter - H*(10) value. Therefore, accepted H*(10) values at reference dose point for both bare DT and SSA prototype were calculated as an average of three measured values after all corrections were applied. Since accuracy of simulated spectral data were confirmed by ROSPEC/SSS measurements the fluence rate and Hp(10) values were derived from H*(10) using computed fluence-to-dose conversion coefficients. The accepted parameters of the fields are listed in Table 4.

Table 4. Accepted Field Parameters

Parameter	Bare DT generator	SSA prototype
Total fluence Φ rate [$s^{-1}.cm^{-2}$]	$1.65 \cdot 10^4$	$9.43 \cdot 10^3$
Ambient dose rate equivalent H*(10) rate [uSv/h]	$2.81 \cdot 10^4$	$1.13 \cdot 10^4$
Personal dose rate equivalent Hp(10) rate [$uSv.cm^2$]	$2.94 \cdot 10^4$	$1.18 \cdot 10^4$

4.0 Test Measurements (Comparison to ^{252}Cf)

The performance of the newly developed neutron field was demonstrated by comparing responses of several neutron instruments and personal dosimeters against the current standardized field generated by NIST-traceable ^{252}Cf spontaneous fission sources.

4.1 Instruments

Neutron instruments selected for testing included two common Remball meters (Hankins 1967), (Ludlum Measurements, Inc n.d.), (Thermo Electron 1991), wide energy neutron detector (Olsher, et al. 2000), (Thermo Fisher Scientific n.d.) and a neutron nuclear criticality detector (Friend 1966). All these instruments employ the same measurement principle - neutron capture in gas proportional counter embedded in polyethylene moderator. Differences of instrument probes are summarized in Table 5.

Table 5. Description of instrument probes

Instrument	Gas Proportional Tube	Moderator
Ludlum 42-31H	Model: LND 25185 1.6 cm x 2.5 cm 2 atm ^{3}He	Polyethylene Sphere 22.5 cm diameter Inner Cd coating
Thermo/Eberline NRD9	Model: NW G-5-1 1.6 cm x 2.5 cm 0.8 atm BF_3	Polyethylene Sphere 22.5 cm diameter Inner Cd alloy shell
Thermo Wendi	Model: LND 252180 2.5 cm x 5 cm 2 atm ^{3}He	Polyethylene Cylinder 23 cm diameter x 21cm long Inner 1.5 cm W powder shell
Hanford NCD	Model: RS-P1-0406-202 1.3 cm x 15 cm 0.5 atm BF_3	Polyethylene Cylinder 12.5 cm diameter x 20 cm long

In order to eliminate variability of signal processing in the different meters and simplify data acquisition, all probes were tested with the same configuration of counting electronics. Detectors were connected via a proportional counter preamplifier (Canberra[1] Model 2006) to Nuclear Instrumentation Module electronics: HV power supply (Canberra Model 9645), Spectroscopy Amplifier (Canberra Model 9615), Amplitude-to-Digital Converter (Canberra Model 9633), and Multi-Channel Analyzer (MCA) (Canberra Model AIM 556) all controlled by Canberra Genie 2000 software installed on a laptop computer. Amplifier shaping constant was set to 0.5uS for high count rate application and the MCA buffer was set for 2048 channels. Amplification gain for each detector type was adjusted to have the entire pulse height distribution not to extend above two thirds of the scale. The countrate was determined as integral number of pulses within region of interest (ROI) divided by live counting time. ROIs were individually set for each type detector, starting at the middle of the valley between the photon/electronic noise and neutron components to the last channel.

All instruments known to be potentially prone to the radiation soaking effect (Mozhayev and Piper 2022) were tested following the same measurement protocol. Prior to calibration, the initial

[1] Mirion Technologies (Canberra), Inc., 800 Research Parkway, Meriden CT

"baseline" level of instrument response is captured in a relatively low rate field (<0.1 mSv/h) and that measurement configuration is used in following instrument control checks. Then, a powered instrument was staged in a high-rate field (~ 50mSv/h) for 15-20 minutes to "stabilize" detector response. The next series of measurements were performed using low and high intensity sources to determine the instrument dead time. Calibration data were acquired in five or more replicate measurements with the same ^{252}Cf source at distance 100 cm, followed by similar series of calibration measurements in generator-produced neutron fields (both bare D-T and SSA prototype). Instrument stability was monitored via frequent control checks conducted in between stabilization, dead-time and calibration measurements.
Instrument measurements are illustrated in Figure 21 and obtained instrument calibration coefficient ratios obtained for bare DT and SSA prototype fields are summarized in Table 6. At the first glance results obtained in the fission-like surrogate spectrum are within 10% tolerance, which is the required accuracy for neutron calibration fields as quoted in the standard (American National Standard 2014).

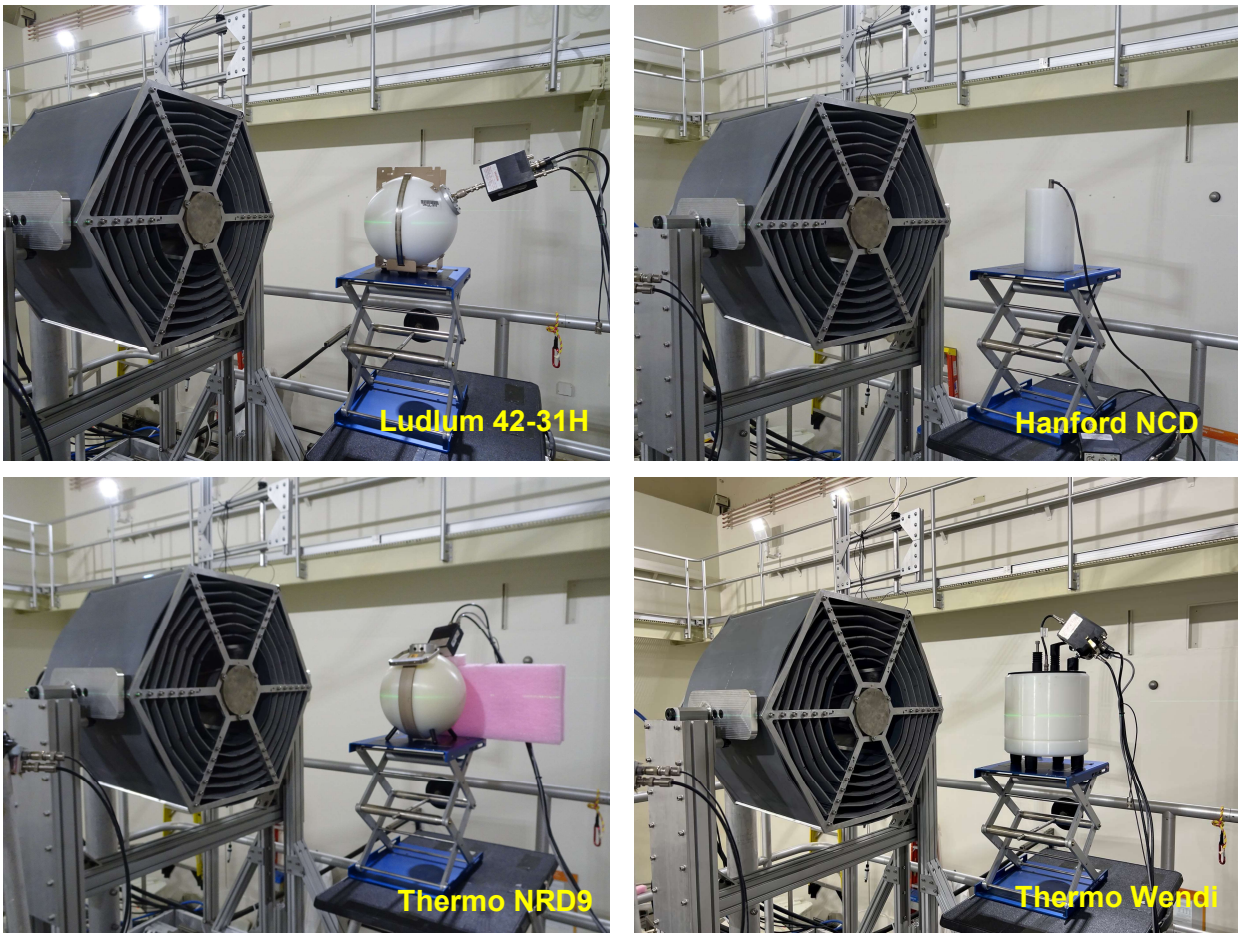

Figure 21. Test measurements with neutron instruments of the SSA prototype field.

Table 6. Instrument calibration coefficient ratios

Instrument	Bare DT / ^{252}Cf (1)	SSA Prototype / ^{252}Cf (2)
Ludlum 42-31H	0.463	0.941
Thermo/Eberline NRD9	0.483	0.926
Thermo Wendi	0.627	0.955
Hanford NCD	0.285	0.976

4.2 Dosimetry

The response of three personal dosimeter types were studied. A Landauer InLight passive dosimeter that includes a single neutron-sensitive, optically stimulated luminescence (OSLN) element of lithium-6 carbonate ($^{6}Li^{2}CO_3$) coated aluminum oxide (Al_2O_3:C) (Passmore and Kirr 2010). These dosimeters were analyzed internally using a Landauer Microstar reader and the net neutron reading attained from subtracting uncoated Al_2O_3:C Element 4 converted counts from those of the OSLN, Element 2. Converted counts correspond to the raw counts adjusted for the detector sensitivity and the calibration factor of the reader (Njiki, et al. 2021). Additional dosimeters consisted of the Mirion, Model DMC2000 GN (Mirion Technologies 2013), single Si-diode active dosimeter and a Thermo Scientific, Model EPD-N2 (Thermo Fisher Scientific 2009), multiple Si-diode active dosimeter (AD). Data for the DMC2000 GN was attained through personal computer (PC) interface through the Mirion DmcUser (ver.1.12.0) software, which yields readings of neutron dose equivalent, Hp(10), as interpreted through calibration against a bare ^{252}Cf reference field. Readout of the EPD-N2 dosimeters employed PC interface using the Thermo Scientific EasyEPD (ver.3.2.2.002) software which yields, among other output, readings of neutron dose equivalent, Hp(10), as interpreted through calibration against an ^{241}Am:Be reference field.

During irradiation to all fields (^{252}Cf , Bare D-T and SSA D-T), dosimeters were mounted on a 40 x 40 x 15cm polymethyl-methacrylate slab phantom to preserve consistent conditions of backscatter and provide albedo dose where necessary. This geometry reflects conditions used during calibration of the dosimeters. Dosimeter irradiations in the SSA prototype field are shown in Figure 22. The dose delivered was varied amongst the dosimeter styles and was suited to balance statistically sufficient anticipated output for each detector with the available irradiator availability. For the OSLN dosimeters, nominal total Hp(10) delivered for ^{252}Cf , Bare DT and SSA DT irradiations were 32, 30 and 12 mSv, respectively. For AD, 54, 15 and 9 mSv were delivered, respectively. It should be noted that electronic dosimeters are expected to respond within ±10% in the energy spectrum they are calibrated to and in other fields results may deviate by 30% or more. Obtained calibration coefficient ratios are summarized in Table 7.

Table 7. Dosimeter calibration coefficient ratios

Dosimeter Type	Parameter	Bare DT / ^{252}Cf (1)	SSA Prototype / ^{252}Cf (2)
Landauer Inlight OSLN	Neutron element response	0.341	1.120
Mirion DMC 2000GN	Neutron response	13.06	1.583
Thermo EPD N2	Neutron Dose	2.972	1.226
	Fast neutron (FN) counts	3.486	1.276
	Thermal neutron (AN) counts	0.460	1.034
	FN/AN ratio	7.558	1.233

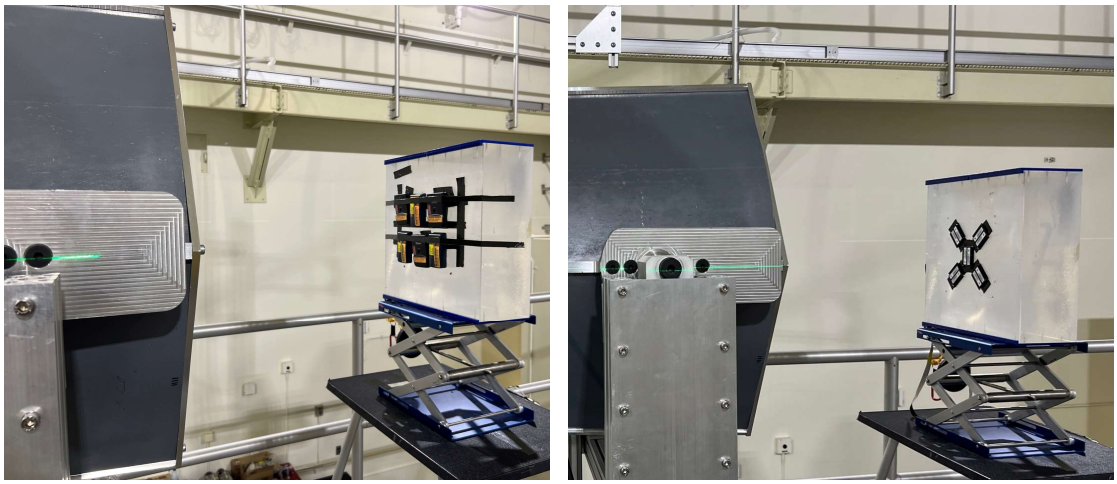

Figure 22. Irradiation of dosimeters on phantom.

5.0 Discussion

Response to the D-T generated SSA prototype neutron field among the various instruments and dosimeters evaluated is notably varied. While differences were expected, this effort was initiated to determine whether such differences are tolerable with such an approach and may be indicative of where improvements might be needed, beneficial or possible. The choice of detectors was intentioned to experience differing instrument construction and sensitivity to both lower- and higher-energy fluence deviations of the SSA field relative to ^{252}Cf reference field.

Response functions (IAEA 2001), (A. V. Mozhayev 2019), (Mirion Technologies 2013), shown in Figure 23, demonstrate the energy-dependent sensitivity of instruments and dosimeters used in the study and provide better understanding of obtained results. Instruments with low sensitivity where the spectra differ, show better agreement between the reference and the SSA fields. For instance, the lower response of the Wendi and Remball at energies less than 10 keV makes them insensitive to the increased scattering apparent in the SSA prototype field. In contrast, the higher sensitivity at 14 MeV results in the Remball and Wendi slightly under responding to the corresponding neutron fluence remainder, which contributes up to 11% of total dose equivalent. Analogously, the NCD decreased sensitivity above 10 MeV and increased low energy response makes it least sensitive to the differences in the spectra.

As this test campaign also examined response of each detector to the bare D-T spectrum, it was conceived that response of detectors listed in Table 6 could be adjusted for the 11% dose fraction of the SSA spectrum exceeding 12.6 MeV. This approach was tested for all instruments by adding to their relative (to Cf-252) response from the SSA their relative (to Cf-252) response from the Bare D-T multiplied by the 0.11. Table 8 illustrates results of such adjustment based on data of Table 6.

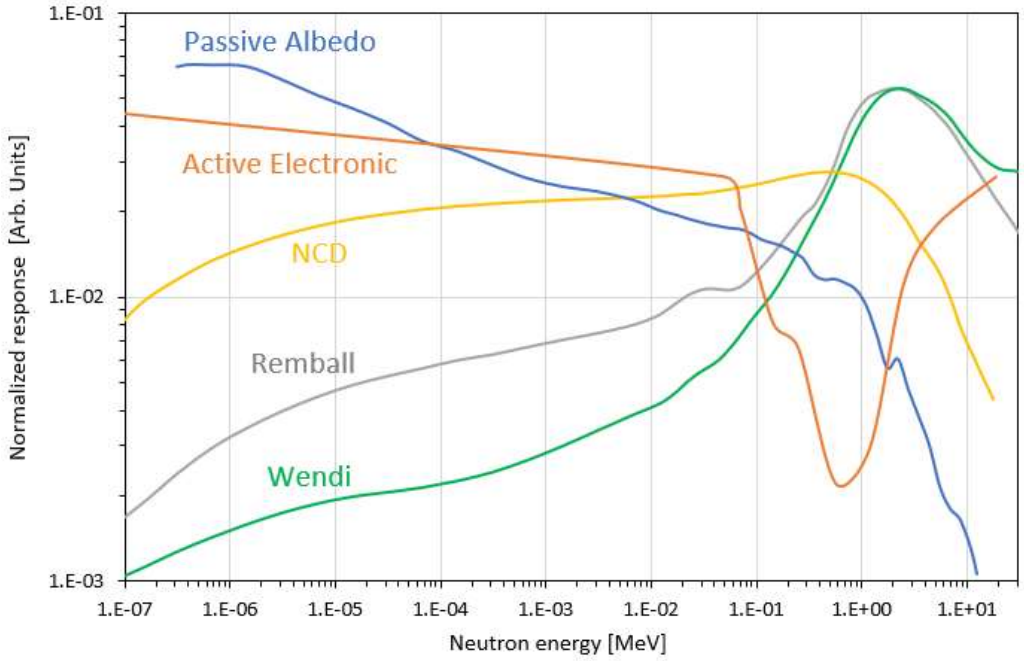

Figure 23. Energy responses of instruments and dosimeters

Table 8. Adjustment of instrument calibration coefficient ratios

Instrument	Bare DT / ^{252}Cf (1)	SSA Prototype / ^{252}Cf (2)	Adjusted (2)*[1+0.11*(1)]
Ludlum 42-31H	0.463	0.941	0.989
Thermo/Eberline NRD9	0.483	0.926	0.975
Thermo Wendi	0.627	0.955	1.021
Hanford NCD	0.285	0.976	1.007

It is noted that the NCD, with its smaller diameter moderator, is not a design commonly used for many conventionally available neutron survey instruments. However, new detectors are being designed to compromise between detection efficiency and ergonomic impact and employ moderators of lesser mass. Therefore, this detector may be indicative of those now or soon to be deployed.

For dosimeters, the response functions shown in the figure suggest that the passive OSL (albedo dosimeter) reading, relative to ^{252}Cf, is driven by its high response in the lower energy ranges – mostly representing the differences due to scattered neutrons - while the AD response – higher at both energy extremes may be sensitive to both the 14 MeV remainder and the additional scatter contributed by the SSA. Dosimeter response adjustments like those made for the 14 MeV remainder to instruments could be more elaborate.

Test measurements with neutron survey instruments and dosimeters demonstrated promising results for recreating a fission-like spectrum by shaping monoenergetic neutrons produced by a D-T generator. While compromises made in the scatterer materials and configuration to the original concept led to expected changes in the spectrum shape, the final result was still satisfactory. Whereas the 14 MeV remainder impact on detector responses can be easily adjusted, the elevated low energy portion of the spectrum due to the increased scatter appears to have a higher influence on dosimeter responses. The absolute fraction of the low energy neutron fluence caused by room scatter at the reference point is like that of the ^{252}Cf field. However, since the shaped field comprises approximately half of the fluence compared to ^{252}Cf, the relative influence of that scatter fraction at the reference point is higher. Reducing this scattered component of the spectrum would be an important but challenging improvement for the surrogate field.

6.0 Conclusions

This effort, intended to practically demonstrate concepts devised in prior works, was accomplished. An earlier conceived means to scatter D-T generated neutrons toward one target spectrum – that of a fission source produced by ^{252}Cf – was designed and built. The as-built design was simulated, taking into consideration compromises in materials availability and added supporting structures in order to determine realistic neutron spectrum. The produced field was evaluated both from the perspective of the neutron fluence spectrum and the resulting dosimetric outcome. Finally, it was tested for practical application by examining response of various health physics instruments and personal monitoring devices in comparison to the response of those devices when exposed to ^{252}Cf.

Despite several compromises in the material, general shape, and supporting structure from that of the original concept, an implementation of the originally conceived spectrum was quite successfully achieved, and the results are promising. Furthermore, the response of several survey-type instruments within the prototype, surrogate fission, reference field are acceptably close to their response in the targeted ^{252}Cf field.

Passive and active personal dosimetry measuring devices evaluated as part of the study resulted in higher response differences, including one example exceeding 30%, relative to the targeted ^{252}Cf field. However, considering the properties of their individual response functions, such differences are expected and not uncommon over many models of neutron-sensitive dosimeters.

Given the promising outcome of this initial demonstration, further study is warranted. Specifically, an evaluation of more and different types of prevalent neutron sensitive instruments and dosimeters would serve to provide the full breadth of response differences possible, given different bases of detection. It is also necessary to understand how reference field reproducibility might be affected in attempting to pair the current SSA design for use with different neutron generator designs. Improvement possibilities should be explored, especially with respect to reducing the 14 MeV remainder and methods for enhancing fluence preservation. Finally, a more comprehensive understanding of normal reference field parameters is needed, including the cross-sectional neutron fluence, energy distribution and angle of neutron incidence at a reference point established with the current configuration – as well as dynamics of those conditions with variability of distance, power variation and aging of a generator. Finally, for applications of such a tool for dosimetry testing, it is essential to understand the gamma and/or X-ray contributions at the reference distance originating from the generator.

DOE-STD-1098-2017, Radiological Control, stresses the application of ANSI N323A to comply with the requirement of Title 10 of the Code of Federal Regulations, Part 835, through the use of neutron radionuclide standards AmBe and bare and D_2O-moderated ^{252}Cf. The effort accomplished by the project provided a proof of concept for creation of a fission-like neutron spectrum leading to the development of the technical basis for an alternative approach to calibrate neutron detection instruments for every site or contractor across the entire DOE complex.

A commercially available neutron generator equipped with an SSA, such as developed, provides a cost-effective solution for replacing the widely used ^{252}Cf sources and improves nuclear safety by minimizing hazards and operational risks associated with nuclear materials.

Besides the fact that a fission-like spectrum is created with no fissionable nuclides, the developed SSA consists of materials that would not lead to the buildup of long-lived activation products, and thus, create no concerns for meeting the requirements of DOE O 420.1C, Facility Safety, and DOE-STD-1027-2018, Hazard Categorization of DOE Nuclear Facilities.

7.0 References

American National Standard. *Radiation Protection Instrumentation Test and Calibration, Portable Survey Instruments.* ANSI N323AB-2013 (Revision and Redesignation of ANSI N323A-1997 and ANSI N323B-2002), ANSI N323AB-2013 (Revision and Redesignation of ANSI N323A-1997 and ANSI N323B-2002), 2014, 1-41.

Benjamin, P. W., C. D. Kemshall, and A. K. Brickstock. *The Analysis of Recoil Proton Spectra.* AWRE 09/68, Atomic Weapons Research Establishment (U.K.), Report AWRE 09/68, 1968.

Bihl, Donald E, Timothy P Lynch, Mark K Murphy, Lynette E Myers, Roman K Piper, and James T Rolph. "Radiation and Health Technology Laboratory Capabilities." PNNL-10354, Rev.2, Pacific Northwest National Laboratory, Richland, Washington, 2005.

Bramblett, R L, R I Ewing, and T W Bonner. "A New Type of Neutron Spectrometer." *Nuclear Instruments and Methods* 9 (1960): 1-12.

Bubble Technology Industries. *BTI Rotating Neutron Spectrometer, ROSPEC, User Manual.* Document Version 25.0, September 23, 2015, 2015.

Chartier, J L, F Posny, and M Buxerolle. "Experimental assembly for the simulation of realistic neutron spectra." *Radiation Protection Dosimetry* 44 (1992): 125-130.

Chichester, David L, and James D Simpson. "Compact accelerator neutron generators." *The Industrial Physicist* 9, no. 6 (Dec 2003): 22-25.

Dubeau, J, S S Hakmana Witharana, J Atanackovic, A Yonkeu, and J P Archambault. "A Neutron Spectrometer using nested moderators." *Radiation Protection Dosimetry* 150, no. 2 (2012): 217-222.

Friend, P C. "Neutron Sensitive Criticality Detector." Technical Manual, BNWL-MA-29, 1966.

Goorley, J. T., et al. "Initial MCNP6 Release Overview." *Nuclear Technology* 180 (2012): 298-315.

Hankins, D E. "A Modified-sphere neutron detector." Report LA-3595, Los Alamos National Laboratory, 1967.

Health Physics Instruments. "Model REM 500 Neutron Survey Meter." Operations and Repair Manual, Rev.A, Goleta, CA, 1998.

IAEA. *Compendium of neutron spectra and detector responses for radiation protection purposes. Supplement to Tecnical Report Series No.318.* Technical Report Series No 403, Vienna: International Atomic Energy Agency, 2001.

Ing, H., S. Djeffal, T. Clifford, L. Li, R. Noulty, and R. Machrafi. "Modification of ROSPEC to Cover Neutrons from Thermal to 18 MeV." *Radiation Protection Dosimetry* 126, no. 1-4 (2007): 350-354.

Ing, H., T. Clifford, T. McLean, W. Webb, T. Cousins, and J. Dhermain. "ROSPEC - A Simple Reliable High Resolution Neutron Spectrometer." *Radiation Protection Dosimetry* 70, no. 1-4 (1997): 273-278.

Kemshall, C. D. *The Use of Spherical Proportional Counters for Neutron Spectrum Measurements.* Atomic Weapons Research Establishment (U.K), Report AWRE 031/73, 1973.

Kim, S I, B H Kim, I Chang, J I Lee, J L Kim, and A S Pradhan. "Response of Six Neutron Survey Meters in Mixed Fields of Fast and Thermal Neutrons." *Radiation Protection Dosimetry* 156, no. 4 (2013): 518-524.

Koltick, D, S McConchie, and E Sword. "Production of a pulseable fission-like neutron flux using a monoenergetic 14 MeV neutron generator and a depleted uranium reflector." *Nuclear Instruments and Methods in Physics Research A* 588 (2008): 414-423.

Ludlum Measurements, Inc. *Model 42-31H Neutron Detector.* n.d. https://ludlums.com/products/all-products/product/model-42-31h (accessed June 2, 2020).

Mirion Technologies. "DMC 2000 GN User's Manual (132616EN-D)." 2 2013.

Mozhayev, A V. "Neutron Criticality Detector: Computational Model and Energy Response." 318RMI-RPT-002, 2019.

Mozhayev, A V, and R K Piper. "Understanding the Radiation Soaking Effect in Neutron Survey Instruments." *Health Physics* 123, no. 1 (2022): 1-10.

Mozhayev, Andrey V, Roman K Piper, Bruce A Rathbone, and Joseph C McDonald. "Investigation of workplace-like calibration fields via a deuterium-tritium (D-T) neutron generator." *Health Physics* 112, no. 4 (2017): 364-375.

Mozhayev, Andrey V, Roman K Piper, Bruce A Rathbone, and Joseph C McDonald. "Moderator design studies for a new neutron reference source based on the D-T fusion reaction." *Radiat. Phys. Chem.* 123 (2016): 87-96.

Njiki, Calvin Didier, Thierry Ndzana Ndah, Germain H. Ben Bolie, Jean Féli Beyala Ateba, Augustin Simo, and Yolande Huguette Ebele Yigbedeck. "Comparison of the Performance of two OSL Readers for the Personal Dose Equivalent Hp(10) Measurement." *Radiation Protection Dosimetry* 193, no. 1 (March 2021): 37-42.

Nunes, J C, W G Cross, and A J Waker. "Feasibility of creating 'CANDU(R)-like' workplace neutron fields in an existing irradiation facility." *Radiation Protection Dosimetry* 72 (1997): 11-20.

Olsher, Richard H., et al. "Wendi: An Improved Neutron REM Meter." *Health Physics* 79, no. 2 (2000): 170-181.

Passmore, Chris., and Mirela Kirr. “Neutron Response Characterisation of an OSL Neutron Dosemeter.” *Radiation Protection Dosimetry*, 2010: 1-6.

Piper, Roman K, Andrey V Mozhayev, Mark K Murphy, and Alan K Thompson. "Beyond Californium - A Neutron Generator Alternative for Dosimetry and Instrument Calibration in the U.S." *Health Physics* 113, no. 3 (2017): 183-194.

Sherman, Steven R, and Bradley D Patton. "Planned Closeout of the Cf-252 Loan/Lease Program." Oak Ridge National Laboratory Report, ORNL/TM-2012/248, 2013.

Thermo Electron. "Neutron REM Detector, Model NRD." Technical Manual, Santa Fe, NM, 1991.

Thermo Fisher Scientific. "EPD-N2 Technical Handbook (EPD/HB/44346/000)." no. 7. 2009.

—. *FHT 762 Wedi-2 Wide-Energy Neutron Detector.* n.d. https://www.thermofisher.com/order/catalog/product/FHT762WENDI2#/FHT762WENDI2 (accessed June 2, 2020).

—. *NRD 9in. Neutron Ball with BF3 Tube.* n.d. https://www.thermofisher.com/order/catalog/product/NRD9#/NRD9 (accessed June 2, 2020).

Pacific Northwest National Laboratory

902 Battelle Boulevard
P.O. Box 999
Richland, WA 99354

1-888-375-PNNL (7665)

www.pnnl.gov